HHS Public Access

Author manuscript

Clin Cancer Res. Author manuscript; available in PMC 2019 December 02.

Published in final edited form as:

Clin Cancer Res. 2018 September 15; 24(18): 4539–4550. doi:10.1158/1078-0432.CCR-18-0327.

Inhibition of EphB4–Ephrin-B2 Signaling Enhances Response to Cetuximab-Radiation Therapy in Head and Neck Cancers

Shilpa Bhatia[1], **Jaspreet Sharma**[1], **Sanjana Bukkapatnam**[1], **Ayman Oweida**[1], **Shelby Lennon**[1], **Andy Phan**[1], **Dallin Milner**[1], **Nomin Uyanga**[1], **Antonio Jimeno**[2], **David Raben**[1], **Hilary Somerset**[3], **Lynn Heasley**[4], **Sana D. Karam**[1]

[1]Department of Radiation Oncology, University of Colorado Denver, Anschutz, Medical Campus, Aurora, Colorado.

[2]Division of Medical Oncology, Department, of Medicine, University of Colorado Denver, Anschutz Medical Campus, Aurora, Colorado.

[3]Department of Pathology, University of Colorado Denver, Anschutz, Medical Campus, Aurora, Colorado.

[4]Department of Craniofacial Biology, University, of Colorado Denver, Anschutz Medical Campus, Aurora, Colorado.

Abstract

Purpose: The clinical success of targeted therapies such as cetuximab and radiotherapy (RT) is hampered by the low response rates and development of therapeutic resistance. In the current study, we investigated the involvement of EphB4–ephrin-B2 protumorigenic signaling in mediating resistance to EGFR inhibition and RT in head and neck cancers.

Experimental Design: We used patient-derived xenograft (PDX) models of head and neck squamous cell carcinoma (HNSCC) and HNSCC cell lines to test our hypothesis. Tumor tissues were subjected to PhosphoRTK array, and Western blotting to detect changes in EphB4–ephrin-B2 targets. mRNA sequencing and microarray data analysis were performed on PDX tumors and

Corresponding Author: Sana D. Karam, University of Colorado Denver, 1665, Aurora Court, Suite 1032, Aurora, CO 80045. Phone: 720-848-0910; Fax: 720-848-0238; sana.karam@ucdenver.edu.

Authors' Contributions

Conception and design: S. Bhatia, J. Sharma, S. Bukkapatnam, S.D. Karam

Development of methodology: S. Bhatia, J. Sharma, A. Jimeno, S.D. Karam

Acquisition of data (provided animals, acquired and managed patients, provided facilities, etc.): S. Bhatia, J. Sharma, A. Phan, D. Milner, N. Uyanga, A. Jimeno, S.D. Karam

Analysis and interpretation of data (e.g., statistical analysis, biostatistics, computational analysis): S. Bhatia, J. Sharma, S. Bukkapatnam, A. Oweida, S. Lennon, A. Phan, H. Somerset, S.D. Karam

Writing, review, and/or revision of the manuscript: S. Bhatia, J. Sharma, A. Oweida, S. Lennon, A. Jimeno, D. Raben, L. Heasley, S.D. Karam

Administrative, technical, or material support (i.e., reporting or organizing data, constructing databases): J. Sharma, S. Bukkapatnam, S.D. Karam

Study supervision: S.D. Karam

S. Bhatia and J. Sharma contributed equally to this article.

Note: Supplementary data for this article are available at Clinical Cancer Research Online (http://clincancerres.aacrjournals.org/).

Disclosure of Potential Conflicts of Interest

No potential conflicts of interest were disclosed.

The costs of publication of this article were defrayed in part by the payment of page charges. This article must therefore be hereby marked *advertisement* in accordance with 18 U.S.C. Section 1734 solely to indicate

HNSCC cell lines, respectively, to determine differences in gene expression of molecules involved in tumor cell growth, proliferation, and survival pathways. Effects on cell growth were determined by MTT assay on HNSCC cells downregulated for EphB4/ephrin-B2 expression, with and without EGFR inhibitor and radiation.

Results: Our data from locally advanced HNSCC patients treated with standard-of-care definitive chemo-RT show elevated EphB4 and ephrin-B2 levels after failure of treatment. We observed significant response toward cetuximab and RT following EphB4–ephrin-B2 inhibition, resulting in improved survival in tumor-bearing mice. Tumor growth inhibition was accompanied by a decrease in the levels of proliferation and prosurvival molecules and increased apoptosis.

Conclusions: Our findings underscore the importance of adopting rational drug combinations to enhance therapeutic effect. Our study documenting enhanced response of HNSCC to cetuximab-RT with EphB4–ephrin-B2 blockade has the potential to translate into the clinic to benefit this patient population.

Introduction

Management of locally advanced head and neck cancer patients, particularly those who are ineligible for cisplatin therapy, relies on combination treatment involving 7 weeks of radiotherapy (RT) with cetuximab, a targeted anti-EGFR therapeutic (1). A phase III trial for locoregionally advanced head and neck cancer patients showed improved overall survival with the addition of cetuximab to RT with some toxicity (2). Only a fraction of HNSCC patients, however, respond to cetuximab-radiation, with an estimated 5-year overall survival of 46% compared with 36% with radiotherapy alone (2). This is partly attributed to loss of sensitivity of tumor cells to EGFR inhibition that develops during treatment and compromises the therapeutic outcome. Concerted research efforts have been made to understand the complex pathways that mediate this underlying treatment resistance (3, 4). Based on data generated in our laboratory and previous studies (5, 6), elevated expression of the Eph-ephrin family of proteins has been hypothesized to play a regulatory role in bypassing some of the therapeutic effects mediated by anti-EGFR therapeutics.

EphB4 belongs to the largest family of receptor tyrosine kinases that interacts with its membrane-bound ligand, ephrin-B2, to trigger prosurvival signaling (7). Our previous data indicate that a feedback loop exists between EphB4–ephrin-B2 and EGFR such that blocking the interaction between EphB4–ephrin-B2 results in decreased p-EGFR and EGFR levels in HNSCCs (5). Other reports in the literature also point toward the presence of a functional interaction between EGFR and EphB4 (6, 8). Consistent with our findings, Park and colleagues used a bioinformatics approach to demonstrate that EGFR and EphB4 functionally interact with each other (8). Based on this, we reasoned that EphB4–ephrin-B2 favors the protumorigenic signaling pathway by altering the sensitivity to targeted anticancer agents and conventional therapies, including radiation. In this study, our data from locally advanced HNSCC patients treated with standard-of-care definitive chemo-RT show high levels of both EphB4 and ephrin-B2 after failure of chemo-RT. This suggests that upregulation of EphB4–ephrin-B2 signaling is responsible for lack of response to therapeutic agents. Therefore, we hypothesized that dual targeting of EphB4–ephrin-B2 will make tumor cells more responsive to an anti-EGFR agent and improve sensitivity of HNSCC

tumors toward RT. We tested this hypothesis *in vitro* and in oral cavity patient-derived xenograft (PDX) models. Our data show significant tumor growth delay and enhanced radiosensitization following combined EphB4–ephrin-B2 inhibition with EGFR inhibitor, resulting in better overall survival in PDX tumors than those treated with the EphB4–ephrin-B2 inhibitor in the presence of cisplatin–RT. The tumor growth inhibition effect observed *in vivo* was accompanied by a decrease in the levels of growth and survival markers and antiapoptotic proteins. An alteration in the circulating IL6 levels was also evident in the tumors subjected to triple combination treatment. These *in vivo* findings were substantiated in cultured HNSCC cells. We observed significant decrease in tumor cell growth in EphB4/ephrin-B2 knockdown cells that were treated with an EGFR inhibitor followed by radiation. Collectively, our data suggest that EphB4–ephrin-B2 and EGFR pathway cooperate with each other to circumvent therapeutic response, resulting in enhanced tumor growth, and apoptotic evasion. Therefore, development and use of combinatorial approaches targeting the Eph-ephrin family of proteins with cetuximab-RT might show promising outcomes in this disease.

Materials and Methods

Cell lines and reagents

The human HNSCC cell line Fadu was obtained from the ATCC. MSK-921 cell line was obtained from Dr. X.J. Wang's lab (University of Colorado, Anschutz Medical Campus, Aurora, CO) and EGFR-resistant human HNSCC cell line 584 was obtained from Dr. Antonio Jimeno (University of Colorado, Anschutz Medical Campus, Aurora, CO). MSK-921 cells were cultured in RPMI-1640 medium with 10% fetal bovine serum and primocin (Invivogen) at 37°C and 5% CO_2. Fadu and 584 cells were maintained in Dulbecco's Modified Eagle's Medium (DMEM) with 10% fetal bovine serum and primocin at 37°C and 5% CO_2. All the cell lines and PDX tumors used in this article were confirmed by STR testing. sEphB4-HSA protein was provided by Vasgene Therapeutics Inc. We and others have previously shown that sEphB4-HSA decreases phospho-EphB4 and phosphoephrin-B2 (5, 9–11). EGFR inhibitors erlotinib and cetuximab were used in cell lines and PDX models, respectively. For comparative effectiveness in *vivo,* we included the cisplatin–RT group to represent standard-of-care therapy. Erlotinib, cetuximab, and cisplatin were obtained from University of Colorado Hospital. Human EphB4 siRNA, ephrin-B2 siRNA, and control siRNA were purchased from Invitrogen.

HNSCC patient samples

Excess, nondiagnostic fresh tumor tissue was collected from HNSCC patients with informed consent at the University of Colorado Hospital in accordance with the protocol approved by the Colorado Multiple Institutional Review Board (COMIRB # 08–0552). The HNSCC patient tumor tissue was collected from patients (i) at the time of the first surgery before treatment with chemo-RT and (2) at the time of the second salvage surgery after they failed chemo-RT and recurred. In this study, we made a comparison of tissue within a group taken at the time of initial diagnosis and then after local failure, at the time of the salvage surgical procedure. Following tumor resection, tumor tissues were examined by a clinical pathologist, and nonnecrotic sections were utilized for research purposes. Normal tonsil

tissue was obtained from the histology core, Gates Center for Regenerative Medicine, Anschutz Medical Campus, Aurora, CO. Tissue was paraffin-embedded and cut as 4 mm-thick sections using a standard protocol.

siRNA transfection

Short-interfering RNA (siRNA) transfection was performed *in vitro* using targeted siRNAs against EphB4 (ID: s243) and ephrin-B2 (ID: 14087). A nonspecific siRNA was used as a negative control. HNSCC cells were transfected in serum-free, antibiotic-free growth medium using Mirus TransIT-TKO Transfection Reagent, according to the manufacturer's instructions. Briefly, cells were transfected using 10 μL TransIT-TKO for a final concentration of 50 nmol/L siRNA. Cells were incubated with the transfection complex for approximately 16 hours, medium was replaced with fresh serum-containing and antibiotic-containing growth medium, and cells were used for further analysis.

MTT assay

The HNSCC cells were plated at a density of 2×10^5 cells/well in a 6-well plate. siRNA transfection using EphB4-siRNA, ephrin-B2-siRNA, and control NS-siRNA (50 nmol/L) was carried out using the protocol described above. Following overnight incubation, media with siRNA complexes were replaced with complete growth medium and cells were treated with an EGFR inhibitor, erlotinib, at 60 nmol/L dose for approximately 16 hours at 37°C. Cells were replated at a density of 1,000 to 2,000 cells/well in a 96-well plate. Following overnight incubation, cells were either left nonirradiated or irradiated with 4 Gy or 8 Gy dose of RT and incubated for 96 to 120 hours. MTT reagent was added to the cells and left at 37°C for 4 hours. Media were aspirated, and formazan MTT crystals were dissolved by adding 100 μL of DMSO reagent. Absorbance was read at 595 nm by using a microplate reader.

Whole-cell lysate preparation

Tumor tissues harvested from control and treatment groups were homogenized in RIPA buffer (Millipore) containing protease inhibitor cocktail (Thermo Fisher Scientific Inc.) and phosphatase inhibitors (Sigma) on ice for 30 minutes. Lysates were collected, and protein concentration was determined using a standard BCA assay as described earlier (5).

Western blotting and antibodies

Protein lysates (20–30 μg) were run onto 10% to 12% SDS–PAGE gels; electrophoresis and blocking were conducted as described (5). Blots were probed overnight at 4°C with respective antibodies. Primary antibodies anti-p-AKT (S473), anti-AKT, anti-Bcl-XL, anti-p-ERK (T202/Y204), anti-ERK, anti-p-STAT3, anti-STAT3, antisurvivin, and anti-β-actin were obtained from Cell Signaling Technology. Anti-EphB4 (clone# m265) and anti- ephrin-B2 antibodies were provided by Vasgene Therapeutics Inc.. Horseradish peroxidase (HRP)-conjugated secondary antibodies were obtained from Sigma.

Irradiation

Radiation treatment was performed in cells and mice with indicated radiation doses using a 160 KVp source RS-2000 (Rad Source Technologies, Inc.) X-ray irradiator at 25 mAmp. The dose rate of 1.24 Gy/minute was used. The irradiator used for these experiments is equipped with a 0.3-mm copper filter. A customized shield exposing only the flank tumors was used to irradiate mice. For quality assurance, we used a Rad Cal model 2086 with a 0.6 cc ion chamber to map the dose every 40 days on average. We measured 5 points at the bottom inside the X-ray irradiator compatible cage and used the reflector when we took our measurements. A Plexiglas device was utilized to duplicate the position of the cage. The acceptance criteria are ±1% of previous reading.

In *vivo* studies

Female athymic nude mice (5–6 weeks old) were purchased from Envigo. All mice were handled and euthanized in accordance with the ethics guidelines and conditions set and overseen by the University of Colorado, Anschutz Medical Campus Animal Care and Use Committee. HNSCC PDX tumors (F8-F12 generation) were obtained from Dr. Antonio Jimeno's lab (University of Colorado, Anschutz Medical Campus). For implantation, tumors were cut into approximately 3 × 3 × 3 mm pieces. Up to 35 mice (70 tumors) were implanted in each experiment. The right and left hind flanks were sterilized, and small incisions were made to create a subcutaneous pocket. Tumor pieces were dipped in Matrigel (BD Biosciences) and inserted into the subcutaneous pocket. Tumor growth was measured using a digital caliper, and tumor volume was calculated using the formula: [(smaller diameter)^2 × (longer diameter)]/2. When tumor volumes reached approximately 100 to 150 mm^3, mice were randomized into 7 groups: (1) PBS, (2) PBS + RT, (3) sEphB4-HSA + RT, (4) cetuximab + RT, (5) cisplatin + RT, (6) sEphB4-HSA + cetuximab + RT, and (7) sEphB4-HSA + cisplatin + RT. The negative control group of mice was administered with PBS intraperitoneally. Loading dose of sEphB4-HSA inhibitor (20 mg/kg; i.p.) and cetuximab (40 mg/kg; i.p.) treatment were initiated 3 days prior to RT treatment. The sEphB4-HSA and cetuximab were then administered concurrently with RT and as maintenance at 20 mg/kg and 10 mg/kg dose, respectively. The maintenance dose of sEphB4-HSA and cetuximab was chosen based on our previous study where we have shown that blocking the interaction between EphB4–ephrin-B2 decreases the levels of p-EGFR and EGFR proteins. We therefore expected a synergistic response between the EGFR inhibitor and EphB4–ephrin-B2 blocking protein. Cisplatin (1 mg/kg; i.p.) was injected 1 hour before RT treatment. This dosing regimen was continued until tumor regrowth was evident. Mice were irradiated 2 times per week at a dose of 5 Gy/fraction for 2 weeks. Tumors were monitored until time of sacrifice as dictated by the animal protocol or until regrowth with a range of 120 to 140 days. The statistical significance on tumor growth curves between control and treatment groups was assessed by ANOVA using the GraphPad Prism 4.0 software. Comparison between 2 groups was made using a *t* test. A *P* value of <0.05 was considered statistically significant. At the end of the experiment, tumors were collected, flash-frozen for Western blot analysis, and formalin fixed for immunohistochemical analysis.

Immunohistochemistry

Immunohistochemical staining was performed on CUHN013 tumors harvested from control and treatment groups implanted using antiproliferating cell nuclear antigen (PCNA) antibody (1:200 dilution, BD Biosciences). This was followed by incubation with biotinylated goat anti-mouse IgG secondary antibody (1:400 dilution; Life Technologies). Tumors from 2 to 3 mice per group were analyzed. For patient specimens ($n = 3$; number of slides analyzed per patient = 5–6), we analyzed EphB4 and ephrin-B2 levels using anti-EphB4 (1:100 dilution, Vasgene Therapeutics Inc.) and anti-ephrin-B2 antibody (1:100 dilution, Vasgene Therapeutics Inc.). Normal human tonsil tissue was used as a negative control. At least 6 to 7 images were captured per group using a 20 × objective on Nikon microscope. Quantification of images was done using ImageJ software.

TUNEL staining

Paraffin-embedded tumor sections were deparaffinized, rehydrated, and subjected to TUNEL staining using *in situ* cell death detection kit (Roche). Images were captured using a Nikon fluorescent microscope. At least 4 to 6 fields were quantified per section by ImageJ software.

Human phospho-RTK array

A human phospho-RTK array kit was purchased from RayBiotech. Tumors were homogenized as described above. Tumor tissue lysates were prepared and incubated with the array as per the manufacturer's instructions. Following the addition of chemiluminescent detection reagents, a signal proportional to the amount of protein bound was detected.

U-plex cytokine/chemokine array

Blood samples were collected from mice via retro-orbital puncture at 96 hours after RT. Plasma was isolated by centrifugation at 3,000 rpm, 15 minutes, 4°C and subjected to U-plex array (Meso Scale Diagnostics) as per the manufacturer's instructions.

RNA extraction and mRNA sequencing

For RNA extraction, PDX tumor tissues were processed and homogenized in 300 mL of QIAzol as described earlier (12). Illumina TruSeq RNA Sample Preparation v2 Guide was used to construct libraries from 1 μg total RNA. The cDNA library was validated on the Agilent 2100 Bioanalyzer DNA-1000 chip. Sequencing was performed as described previously (12). The bioinformatics strategy outlined in the Keysar and colleagues was used (12).

Statistical analysis

The experiments were performed in duplicate or triplicate and repeated 2 to 3 times. Quantitative analyses were performed using the Student *t* test or ANOVA. A P value of <0.05 was considered statistically significant.

Results

HNSCC patients who failed concurrent chemo-RT show upregulated levels of EphB4 and ephrin-B2

We examined tumor samples biopsied from HNSCC patients (i) at the time of the first surgery before treatment with chemo-RT and (ii) at the time of the second salvage surgery after they failed chemo-RT and recurred. We made a comparison of tissue within a group taken at the time of initial diagnosis and then after local failure, at the time of the salvage surgical procedure. To correlate our gene of interest and treatment resistance, we performed immunohistochemical analysis on these patient specimens using anti-EphB4 and anti-ephrin-B2 antibodies. Our data show basal expression of both EphB4 and ephrin-B2 present in tumor tissues at the time of initial diagnosis (Fig. 1). The expression was mainly confined to the cell membrane. Normal tonsil tissue was used as negative control and did not show significant expression of these proteins (Fig. 1). However, analysis of tissues harvested after treatment failure indicates that levels of EphB4 and ephrin-B2 were upregulated to approximately 20% to 25% compared with tissue analyzed at the time of initial diagnosis, where EphB4 and ephrin-B2 levels range between 7% and 10% (Fig. 1), implicating that this receptor-ligand pair may have a role to play in resistance to the treatment regimen.

Blockade of EphB4–ephrin-B2 receptor-ligand axis enhances response to cetuximab-RT and improves survival in mice bearing HNSCC PDX tumors

To test our hypothesis *in vivo,* we chose 2 PDX tumors—CUHN013 and CUHN004. Both the CUHN013 and CUHN004 PDXs are derived from patients with heavy smoking history (12). CUHN013 is derived from primary site and CUHN004 is derived from relapsed tumor. They have elevated expression of EphB4 (5), ephrin-B2 (11), and EGFR (Supplementary Fig. S1) and thus represent valid models to test our hypothesis (13). Mice were also treated with cisplatin and RT in the absence and presence of the EphB4–ephrin-B2 inhibitor, sEphB4-HSA. The purpose of including the standard of care arm, cisplatin + RT, is to make a direct comparison with the cetuximab + sEphB4-HSA + RT treatment arm. Our in vivo data show that when CUHN013 and CUHN004 PDX tumors were treated with cetuximab and sEphB4-HSA followed by RT treatment (5 Gy × 4 fractions), tumors grew significantly slower compared with control and other experimental groups (Fig. 2A–D). Overall, triple combination with cetuximab, sEphB4-HSA, and RT decreased the tumor growth by 2.6-fold in CUHN013 (Fig. 2A) and 3.1-fold in CUHN004 tumors compared with the cetuximab–RT group on days 109 to 112 after treatment (Fig. 2B and D). Dual therapy with sEphB4-HSA-RT, cisplatin–RT, or cetuximab–RT resulted in regrowth after an initial responsive phase of approximately 30, 20, and 110 days, respectively, for CUHN013 tumors (Fig. 2A; Supplementary Fig. S2A) and 32, 21, and 100 days for CUHN004 tumors (Fig. 2C; Supplementary Fig. S2B). Triple therapy with either cisplatin-sEphB4-HSA-RT or cetuximab-sEphB4-HSA-RT yielded an average tumor control for 31 and 116 days in the CUHN013 mice (Fig. 2A; Supplementary Fig. S2A) and 42 and 125 days in the CUHN004 mice, respectively (Fig. 2C; Supplementary Fig. S2B). In CUHN013 tumor-bearing mice, 40% of the mice survived to day 140 with cetuximab-RT-sEphB4-HSA compared with 20% with cetuximab-RT (Fig. 2E). In CUHN004 tumors, 80% of the mice that received cetuximab-RT-sEphB4-HSA survived at the last time point analyzed compared with 20% in

the cetuximab–RT cohort (Fig. 2F). The median survival was not reached for the CUHN004 mice treated with cetuxi-mab–RT–sEphB4-HSA and averaged 120 days for cetuximab–RT cohort (Fig. 2F). For combination cisplatin-based therapy, there was no improvement in tumor control or median overall survival between cisplatin–RT and cisplatin-sEphB4-HSA-RT in the CUHN013 tumors (Fig. 2E; Supplementary Fig. S2C). In CUHN004 tumors, the cisplatin–RT treatment suffered significant toxicity, weight loss, and premature death in the context of retro-orbital blood collection, so definitive conclusions cannot be drawn. However, triple therapy with cisplatin–RT–sEphB4-HSA increased median survival to 103 days compared with 23 days with cisplatin + RT (Fig. 2F; Supplementary Fig. S2D).

To understand the treatment response of CUHN004 and CUHN013 PDX tumors, mRNA seq analysis was conducted on F1 PDX tumor tissue. We examined baseline levels of specific genes that have been reported to mediate EphB4–ephrin-B2 signaling and EGFR inhibitor resistance such as MAPK1, AKT, JAK2, STAT3, SHP1, SHP2, Bcl-XL, survivin, SOCS3, and the angiogenic proteins VEGFA and VEGFC (5, 14–21). High levels of gene expression of downstream targets of EphB4–ephrin-B2 signaling such as MAPK1, survivin, STAT3, AKT1, AKT2, VEGFA, and VEGFC are observed in CUHN004 at baseline compared with CUHN013 PDX tumors (Fig. 2G).

Enhanced antitumor response observed in PDX tumors following combined EGFR and EphB4–ephrin-B2 inhibitor treatment with radiation is associated with decreased tumor proliferation and increased apoptotic cell death

We assessed the levels of PCNA in control and experimental CUHN013 tumors to determine the effect of treatment on tumor cell proliferation. We observed significant decrease in the percentage of cells expressing PCNA in cetuximab-treated groups following addition of sEphB4-HSA with RT compared with their treatment controls (Fig. 3A and C). The percentage of PCNA-positive cells decreased from approximately 43.78% in control to 34.99% in sEphB4-HSA + RT, and 28% in cetuximab + RT. Adding sEphB4-HSA to cetuximab + RT reduced the percentage of PCNA-positive cells further to 23% (Fig. 3A and C). In addition, we subjected CUHN013 tumor sections to TUNEL staining to determine the extent of apoptosis following addition of sEphB4-HSA to cetuximab + RT treatment. Our data revealed that the percentage of TUNEL-positive cells increased following treatment with sEphB4-HSA (27%), compared with the PBS group (4.4%) (Fig. 3B and D). Combining EphB4–ephrin-B2 inhibitor with cetuximab and RT increased TUNEL staining to approximately 44% compared with other groups, indicative of an enhanced apoptotic effect (Fig. 3B and D).

To substantiate IHC/IF data, we also analyzed levels of key proteins known to promote tumor growth and survival by Western blotting. Our data show a decrease in the levels of p-ERK, ERK, and survivin in CUHN013 tumors treated with EphB4–ephrin-B2 inhibitor and cetuximab in the presence of RT (Fig. 3E). In CUHN004 tumors, key target molecules that were decreased upon triple combination involving cetuximab treatment include p-AKT, p-ERK, ERK, and Bcl-XL (Fig. 3F), suggesting that the anticancer effects observed in these cohorts are predominantly associated with coordinated inhibition of tumor growth promoting and antiapoptotic pathways.

To explore differences in the phosphorylation of downstream targets that could account for the response when sEphB4-HSA is added to cetuximab-RT, tumor tissues were subjected to phospho-array analysis. Our data show a decrease in p-FAK levels in tumors treated with sEphB4-HSA + cetuximab + RT combination compared with the sEphB4-HSA + RT group (Fig. 3G). Finally, to determine the effect of sEphB4-HSA to cetuximab-RT on inflammatory cytokines, we analyzed circulating levels of IL6 in CUHN013 and CUHN004 tumor-bearing mice. IL6 acts a regulator of key signaling pathways including proliferation, survival, apoptosis, angiogenesis, and metastatic spread (22). We observed a significant decrease in levels of IL6 particularly in CUHN013 tumors treated with sEphB4-HSA + cetuximab and RT compared with other groups (Fig. 3H). IL6 has been shown to trigger a prolonged response to EGFR via the association of the IL6 receptor with EGFR (23). This leads to EGFR-dependent rephosphorylation of STAT3, which fails to respond to the inhibitory signal by SOCS3, resulting in prolonged EGFR activation. Consistent with IL6 data, we observed a decrease in the levels of p-STAT3 in the sEphB4-HSA + cetuximab + RT group compared with the sEphB4-HSA + RT or cetuximab + RT (Fig. 3I). A similar trend was not evident in CUHN004 tumors (Fig. 3I).

Dual EphB4/ephrin-B2 and EGFR inhibition with radiation results in decreased tumor growth in HNSCC cells *in vitro*

To recapitulate the *in vivo* findings, we performed MTT assays using 3 different HNSCC cell lines—MSK-921, Fadu, and 584. These cell lines possess high levels of both EphB4 and ephrin-B2 and display differences in sensitivity to EGFR inhibitor (5,24,25). Therefore, they represent ideal model systems to test the underlying hypothesis whether inhibiting EphB4–ephrin-B2 can make these cells more responsive to EGFR inhibitor and radiation treatment. Our data show that treatment of Fadu cells with an EGFR inhibitor, erlotinib, did not show significant reduction in tumor cell growth. However, when EphB4 or ephrin-B2 is knocked down in these cells, they respond better to EGFR inhibition as evident by decrease in tumor cell growth to approximately 40% (Fig. 4A). Importantly, when Fadu cells downregulated for EphB4/ephrin-B2 expression were exposed to erlotinib and RT, they showed pronounced reduction in tumor growth to approximately 19% (Fig. 4A). In addition, we used another HNSCC cell line, 584, which is known to be resistant to EGFR inhibitor (25). As expected, treatment with erlotinib failed to show tumor cell growth reduction in584 cells (Fig. 4B). This trend in cell growth was altered, and 584 cells became more sensitive to erlotinib when EphB4 or ephrin-B2 were silenced using targeted siRNAs as evident by reduction in cell growth to approximately 60% (Fig. 4B). Furthermore, treating the knockdown cells with erlotinib also made these cells more responsive to the radiation treatment as evident by significant reduction in tumor cell growth to approximately 35% to 40% in the irradiated group compared with the nonirradiated controls (Fig. 4B). MSK-921 cells showed similar response to EGFR inhibition and RT treatment following EphB4 downregulation with decrease in cell growth to approximately 35% (Fig. 4C).

To understand the differential response, we analyzed the previously published Affymetrix microarray data (26) on HNSCC cell lines (Fig. 4D). Our analysis revealed that most of the genes that support tumor cell survival, growth, and proliferation were differentially expressed in these HNSCC cells—MSK-921, Fadu, and 584. MSK-921 demonstrated least

sensitivity to both EGFR inhibitor and radiation by itself in the MTT assay. This could be partly associated with high expression of genes that regulate tumor growth, progression, and apoptotic cell death such as STAT3, EGFR, Bcl-XL, and AKT2 (Fig. 4D) present in this cell line compared with others. 584 cells, on the other hand, had comparable levels of AKT2, VEGFA, and Bcl-XL as Fadu (Fig. 4D).

Discussion

Therapeutic resistance is a major roadblock in the field of cancer medicine that compromises the efficacy of available treatment regimens. Understanding these resistance mechanisms that precede clinical intervention or in some cases come into play after the course of treatment is an area of extreme significance. EGFR has been utilized as a prime target for numerous human malignancies, including head and neck cancer. However, clinical data suggest that patients treated with targeted EGFR inhibitors, such as cetuximab, do not achieve maximal benefit (2). This suggests potential involvement of redundant or compensatory tumor survival pathways that come into action and blunt the antitumor effects of a potent targeted therapeutic as cetuximab. In this scenario, targeting one protein alone may not be efficacious and necessitates adopting a rationalized two-pronged approach to maximize the therapeutic response. Based on data generated in our laboratory and previous studies (5, 6), dysregulated levels of the Eph-ephrin family of proteins has been hypothesized to play a regulatory role in bypassing the therapeutic effects mediated by the anti-EGFR therapeutics and RT. We have previously demonstrated that blockade of EphB4–ephrin-B2 interaction using sEphB4-HSA decreases tumor growth in HNSCC PDX tumors compared with the control group (5). These tumors eventually regrew even in the presence of continued administration of the inhibitor (5). In the current study, we tested the concept whether combined inhibition of EphB4–ephrin-B2 and EGFR can enhance the sensitivity of PDX tumors to RT and observed that blockade of EphB4–ephrin-B2 increased sensitivity of HNSCC tumors to both EGFR inhibitor and radiation by inhibiting tumor cell proliferation and by enhancing apoptotic cell death. The phenomenon of therapeutic resistance has been observed in other cancer models. Isoyama and colleagues demonstrated that acquired resistance to phosphatidylinositol 3-kinase (PI3K) inhibitors was mediated by the elevation of the insulin-like growth factor 1 receptor (IGF1R) pathway in multiple cancers and that the targeted inhibition of IGF1R reversed the acquired PI3Ki resistance phenotype (27).

In our study, we found significant reduction in tumor growth and improved survival in PDX tumors subjected to RT following EGFR inhibition in combination with EphB4–ephrin-B2 blockade. Importantly, during monitoring these tumor-bearing mice for approximately 4.5 months, we observed differences in response to the treatment between CUHN013 and CUHN004 tumors. In CUHN013 tumors, no significant differences were observed in terms of tumor growth delay effect between sEphB4-HSA or cisplatin intervention with RT and triple combination involving cisplatin. However, combining cetuximab-RT with EphB4–ephrin-B2 inhibitor showed significant antitumor response in these tumors. Importantly, a partial durable response was evident in triple combination groups with anti-EGFR inhibitor that was maintained for an extended period of 4.5 months. The difference in response is attributed to the distinct molecular profile of these PDX tumors. Our mRNA seq analysis performed on F1 PDX tumors shows a differential pattern of expression of genes involved in

survival pathways, apoptosis, and angiogenesis. Some of these have been well established to be downstream targets of both the EGFR and EphB4–ephrin-B2 signaling axes. Many of the known targets for both EphB4–ephrin-B2 signaling and cetuximab, such as AKT, MAPK/ERK, STAT3, survivin, and members of the VEGF pathway (5, 16–21, 28, 29), are highly upregulated in CUHN004 tumors compared with CUHN013 tumors. These can potentially serve as candidate biomarkers for response to such combination therapies pending validation in clinical trials. Upon further validation, we observed decrease in the levels of some of these proteins, including p-AKT, p-ERK, ERK, Bcl-XL, and survivin in triple combination groups by Western blot analysis. In addition, we noticed reduction in phospho levels of kinases such as FAK in the cetuximab cohort combined with sEphB4-HSA and RT in CUHN013 tumors. FAK has been reported to act downstream of other tyrosine kinases including EphB4 and regulate cellular adhesion, migration, proliferation, and survival in various types of tumor models (30–32). Thus, our findings suggest that decrease in tumor growth evident in the triple combination group is a resultant of the coordinated action on FAK that is functioning downstream of the EphB4–ephrin-B2 and EGFR pathways.

The Eph-ephrin family of proteins, in particular, ephrin-B2, has been historically linked to pathologic angiogenesis by engaging in a cross-talk with the components of tumor microenvironment (TME; refs. 16, 21). The tumor microenvironment is typically enriched with tumor-promoting cytokines that plays a key role in cancer pathogenesis. IL6 is one of the protumorigenic cytokines that support tumor progression by influencing tumor cell proliferation, survival, apoptosis, angiogenesis, and metastasis (22). To understand how the triple combination approach utilized in this study affected tumor growth by modulating profile of inflammatory cytokines, we examined levels of IL6 in plasma samples of mice injected with sEphB4-HSA + RT by itself or in combination with cetuximab. InCUHN013 PDX tumor-bearing mice subjected to EphB4–ephrin-B2 inhibitor in the presence of cetuximab-RT, we observed decrease in the levels of IL6 compared with other groups. IL6 has been shown to trigger a prolonged response to EGFR via the association of the IL6 receptor with EGFR (23). This leads to EGFR-dependent rephosphorylation of STAT3, which fails to respond to the inhibitory signal by SOCS3, resulting in prolonged EGFR activation. Combination therapy with inhibitors of EGFR kinase activity and agents that inhibit STAT3, such as sEphB4-HSA (5), has been suggested to have enhanced synergy. Because we observed a differential response in PDX tumors, we believe that the response in CUHN013, in particular, is driven by EGFR inhibition. Noteworthy, the decrease in IL6 and STAT3 is more substantial in CUHN013; therefore, we hypothesize that the IL6-EGFR-STAT3 axis is driving tumor progression in this tumor and that the synergistic effects between sEphB4-HSA and cetuximab are targeting this axis. Our data are also in agreement with a recent study demonstrating an association between IL6 and response to dasatinib (a tyrosine kinase inhibitor targeting EphB4) and cetuximab in cetuximab-resistant head and neck cancer (33). These findings are also important in light of the fact that IL6 has been reported to act as a potential predictor of antitumor response following cetuximab-based therapy in locally advanced head and neck cancer patients (34).

Overall, our findings underscore the importance of using rational combinations that are more personalized in nature and design to allow maximal clinical benefit and avoid undesirable toxicity. One would expect the HPV-negative status to have an impact on the proposed

treatment outcome. We have in fact evaluated the efficacy of an EphB4–ephrin-B2 inhibitor, sEphB4-HSA, in the absence and presence of radiation in PDX tumors derived from both HPV-negative and HPV-positive patients in a previous study (5). We observed that although inhibition of EphB4–ephrin-B2 signaling radiosensitized both HPV-negative and HPV-positive PDX tumors, the magnitude of difference, in the presence of radiation, was much lower in the HPV-positive tumors (5). Perhaps much of this is driven by the fact that HPV^+ tumors are exquisitely radiosensitive, and it is difficult to assess the effect of a radiosensitizer in that setting. In a locally advanced setting, in the context of HPV status and response to cetuximab, the data are conflicting (35–49). We are awaiting the results of RTOG 1016 to answer this important question. For HPV-negative cancers, in numerous studies the comparative effectiveness of cetuximab versus cisplatin remains controversial (35–46, 48, 49). The perception is that cisplatin is superior to cetuximab, at least for high-risk oropharyngeal cancer. For oral cavity cancers, from which tumors in this study were derived, little to no data exist on the topic. RTOG 0920 recently closed and should help address the question of whether the addition of cetuximab to radiation improves survival outcomes for postoperative patients with intermediate-risk pathologic features. The PDX tumors used in our study were derived from the primary site or relapsed tumor (oral cavity) with aggressive tumor pathology. We show a differential response to therapy between the two. Both seem to show better response to cetuximab-radiation than cisplatin-radiation. The addition of sEphB4-HSA appeared to show synergistic effect with cetuximab-RT in both tumors. Some synergy was noted with cisplatin–RT in CUHN004, but not in CUHN013, suggesting different biological mechanisms. As far as EGFR mutations are concerned, they rarely occur in HNSCCs (50, 51), results we have also confirmed in the TCGA analysis. Unlike lung adenocarcinoma, there are no missense mutations noted in HNSCC.

Furthermore, in the context of cetuximab–RT regimen in HNSCC patients, the Bonner trial identified a survival benefit in patients administered with cetuximab combined with radiation (RT) over radiation alone in patients with locoregionally advanced cancer (2). This confirmed a favorable interaction of cetuximab with RT. Conversely, RTOG-0522 (Randomized Phase III Trial of Concurrent Accelerated Radiation and Cisplatin versus Concurrent Accelerated Radiation, Cisplatin, and Cetuximab [C225] [Followed by Surgery for Selected Patients] for Stage III and IV Head and Neck Carcinomas) did not demonstrate a survival benefit with the addition of cetuximab to RT and cisplatin in the primary head and neck cancer treatment setting (52). The current data published in the definitive primary treatment setting of locally advanced HNSCCs comparing cisplatin–RT with cetuximab–RT have mostly yielded conflicting conclusions (35–49, 53). The only available randomized controlled trial evidence comparing concurrent cisplatin to cetuximab in the setting of definitive CRT is a phase II trial that reported that there was no difference between the 2 arms in survival or disease-free progression. Additional randomized controlled trials are ongoing (54–56). These studies, however, including the Bonner trial, are done in the context of oropharyngeal cancer. In the context of oral cavity cancer, from which our PDX tumors and tissue were derived, little to no comparative data exist on the benefit of adding cetuximab as a radiosensitizer in the adjuvant setting. In the high-risk setting (extranodal extension or positive margin), adjuvant cisplatin–RT is considered standard of care, but the benefit of adding cisplatin to radiation in this setting is modest and is accompanied by

incremental toxicity. Additionally, a substantial cohort of patients exists that does not tolerate cisplatin during radiation. In the phase II RTOG 0234 clinical trial (57), where 46% of the patients were oral cavity cancer, it was shown that the addition of cetuximab to postoperative chemoradiotherapy was feasible and tolerated. A survival advantage was also observed for the docetaxel regimen suggesting that rational combinations with EGFR inhibitors are more likely to yield synergistic effects in the setting of radiosensitization. Based on previous reports suggestive of a functional interaction between EGFR and EphB4 (6, 8) and our data showing that blockade of the interaction between EphB4–ephrin-B2 results in decreased p-EGFR and EGFR levels in HNSCCs (5), we hypothesized a synergistic effect between the two.

Given that cisplatin is standard-of-care therapy, we made an attempt to compare the radiosensitization effect of combination of blockade of the EphB4–ephrinB2 interaction with either cetuximab or cisplatin. Preclinically, we used 2 aggressive PDX models (CUHN013 andCUHN004) derived from patients that had failed (locoregionally and later distantly). Tissue for PDX implantation was taken at the time of surgical resection (primary resection for CUHN013, salvage resection for CUHN004). Our data unexpectedly showed that in both PDX models (i) cetuximab is a superior radiosensitizer than cisplatin and (ii) sEphB4-HSA showed improved synergy with cetuximab to enhance radiosensitization than with cisplatin. Unfortunately, we do not have a reliable and definitive biomarker that would help to decide whether these patients should receive cetuximab or cisplatin. While definitive chemoradiation (CRT) is the standard of care for oropharyngeal HNSCCs, we hesitate extrapolating into that disease setting as we are likely dealing with different biology. Multiple studies have shown that oral cavity cancers have different drivers of oncogenesis (58–62). Our data demonstrate for the first time that patients that failed to respond to definitive chemo-RT have upregulated levels of both EphB4 and ephrin-B2. This information can be highly relevant in the near future to stratify the patients and adopt a personalized therapeutic approach. In fact, the EphB4–ephrin-B2 inhibitor sEphB4-HSA is currently being tested in clinical trials for different human cancers (NCT0164232, NCT02799485, NCT02717156, and NCT02767921). Based on our findings, we hypothesize that in a locally advanced setting, patients with oral cavity cancers, heavy smoking history, and aggressive tumor biology might be more likely to benefit from the proposed treatment in the current study. These data should hopefully inform the design of clinical trials in HPV-negative, smoking driven, locally advanced HNSCCs. Importantly, mechanistic understanding of how these combination therapies works is equally important and our data shed light on the key molecular components that are altered in response to the EphB4–ephrin-B2 inhibitor administered with anti-EGFR therapeutic and RT. We believe that the implications of this study will be profound and far reaching in the field, which is plagued by the lack of effective therapies to provide durable and specific response for the head and neck cancer patient population.

Supplementary Material

Refer to Web version on PubMed Central for supplementary material.

Acknowledgments

S.D. Karam is supported by the Paul Calabresi Career Development Award for Clinical Oncology (K12, CA086913), RSNA grant RSD1713, Golfer's against Cancer, and a Cancer League of Colorado grant. The authors acknowledge Dr. Parkash Gill (University of Southern California, Los, Angeles, California) and Vasgene Therapeutics Inc. (Los Angeles, California) for providing sEphB4-HSA protein.

References

1. Adelstein D, Gillison ML, Pfister DG, Spencer S, Adkins D, Brizel DM, et al. NCCN guidelines insights: head and neck cancers, version 2.2017. J Natl Compr Canc Netw 2017;15:761–70. [PubMed: 28596256]
2. Bonner JA, Harari PM, Giralt J, Cohen RB, Jones CU, Sur RK, et al. Radiotherapy plus cetuximab for locoregionally advanced head and neck cancer: 5-year survival data from a phase 3 randomised trial, and relation between cetuximab-induced rash and survival. Lancet Oncol 2010;11: 21–8. [PubMed: 19897418]
3. Cooper JB, Cohen EE. Mechanisms of resistance to EGFR inhibitors in head and neck cancer. Head Neck 2009;31:1086–94. [PubMed: 19378324]
4. Quesnelle KM, Wheeler SE, Ratay MK, Grandis JR. Preclinical modeling of EGFR inhibitor resistance in head and neck cancer. Cancer Biol Ther 2012;13:935–45. [PubMed: 22785204]
5. Bhatia S, Hirsch K, Sharma J, Oweida A, Griego A, Keysar S, et al. Enhancing radiosensitization in EphB4 receptor-expressing head and neck squamous cell carcinomas. Sci Rep 2016;6:38792. [PubMed: 27941840]
6. Masood R, Kumar SR, Sinha UK, Crowe DL, Krasnoperov V, Reddy RK, et al. EphB4 provides survival advantage to squamous cell carcinoma of the head and neck. Int J Cancer 2006;119:1236–48. [PubMed: 16615113]
7. Pasquale EB. Eph receptors and ephrins in cancer: bidirectional signalling and beyond. Nat Rev Cancer 2010;10:165–80. [PubMed: 20179713]
8. Park CY, Krishnan A, Zhu Q, Wong AK, Lee YS, Troyanskaya OG. Tissue-aware data integration approach for the inference of pathway interactions in metazoan organisms. Bioinformatics 2015;31:1093–101. [PubMed: 25431329]
9. Scehnet JS, Ley EJ, Krasnoperov V, Liu R, Manchanda PK, Sjoberg E, et al. The role of Ephs, Ephrins, and growth factors in Kaposi sarcoma and implications of EphrinB2 blockade. Blood 2009;113:254–63. [PubMed: 18836096]
10. Oweida A, Lennon S, Calame D, Korpela S, Bhatia S, Sharma J, et al. Ionizing radiation sensitizes tumors to PD-L1 immune checkpoint block¬ade in orthotopic murine head and neck squamous cell carcinoma. Oncoimmunology 2017;6:e1356153.
11. Oweida A, Bhatia S, Hirsch K, Calame D, Griego A, Keysar S, et al. Ephrin-B2 overexpression predicts for poor prognosis and response to therapy in solid tumors. Mol Carcinog 2017;56:1189–96. [PubMed: 27649287]
12. Keysar SB, Astling DP, Anderson RT, Vogler BW, Bowles DW, Morton JJ, et al. A patient tumor transplant model of squamous cell cancer identifies PI3K inhibitors as candidate therapeutics in defined molecular bins. Mol Oncol 2013;7:776–90. [PubMed: 23607916]
13. Keysar SB, Le PN, Anderson RT, Morton JJ, Bowles DW, Paylor JJ, et al. Hedgehog signaling alters reliance on EGF receptor signaling and mediates anti-EGFR therapeutic resistance in head and neck cancer. Cancer Res 2013;73:3381–92. [PubMed: 23576557]
14. Ferguson BD, Liu R, Rolle CE, Tan YH, Krasnoperov V, Kanteti R, et al. The EphB4 receptor tyrosine kinase promotes lung cancer growth: a potential novel therapeutic target. PLoS One 2013;8:e67668.
15. Kwak H, Salvucci O, Weigert R, Martinez-Torrecuadrada JL, Henkemeyer M, Poulos MG, et al. Sinusoidal ephrin receptor EPHB4 controls hematopoietic progenitor cell mobilization from bone marrow. J Clin Invest 2016;126:4554–68. [PubMed: 27820703]

16. Sawamiphak S, Seidel S, Essmann CL,Wilkinson GA, Pitulescu ME, Acker T, et al. Ephrin-B2 regulates VEGFR2 function in developmental and tumour angiogenesis. Nature 2010;465:487–91. [PubMed: 20445540]
17. Zuo Q, Shi M, Li L, Chen J, Luo R. Development of cetuximab-resistant human nasopharyngeal carcinoma cell lines and mechanisms of drug resistance. Biomed Pharmacother 2010;64:550–8. [PubMed: 20630698]
18. Pradeep S, Huang J, Mora EM, Nick AM, Cho MS, Wu SY, et al. Erythropoietin stimulates tumor growth via EphB4. Cancer Cell 2015; 28:610–22. [PubMed: 26481148]
19. Abengozar MA, de Frutos S, Ferreiro S, Soriano J, Perez-Martinez M, Olmeda D, et al. Blocking ephrinB2 with highly specific antibodies inhibits angiogenesis, lymphangiogenesis, and tumor growth. Blood 2012;119: 4565–76. [PubMed: 22446484]
20. Zhang G, Brady J, Liang WC, Wu Y, Henkemeyer M, Yan M. EphB4 forward signalling regulates lymphatic valve development. Nat Commun 2015;6: 6625. [PubMed: 25865237]
21. Wang Y, Nakayama M, Pitulescu ME, Schmidt TS, Bochenek ML, Sakaki-bara A, et al. Ephrin-B2 controls VEGF-induced angiogenesis and lymphangiogenesis. Nature 2010;465:483–6. [PubMed: 20445537]
22. Kumari N, Dwarakanath BS, Das A, Bhatt AN. Role of interleukin-6 in cancer progression and therapeutic resistance. Tumour Biol 2016;37: 11553–72. [PubMed: 27260630]
23. Wang Y, van Boxel-Dezaire AH, Cheon H, Yang J, Stark GR. STAT3 activation in response to IL-6 is prolonged by the binding of IL-6 receptor to EGF receptor. Proc Natl Acad Sci U S A 2013;110:16975–80. [PubMed: 24082147]
24. Kalinowski FC, Giles KM, Candy PA, Ali A, Ganda C, Epis MR, et al. Regulation of epidermal growth factor receptor signaling and erlotinib sensitivity in head and neck cancer cells by miR-7. PLoS One 2012;7: e47067.
25. Marshall ME, Hinz TK, Kono SA, Singleton KR, Bichon B, Ware KE, et al. Fibroblast growth factor receptors are components of autocrine signaling networks in head and neck squamous cell carcinoma cells. Clin Cancer Res 2011;17:5016–25. [PubMed: 21673064]
26. Frederick BA, Helfrich BA, Coldren CD, Zheng D, Chan D, Bunn PA Jr, et al. Epithelial to mesenchymal transition predicts gefitinib resistance in cell lines of head and neck squamous cell carcinoma and non-small cell lung carcinoma. Mol Cancer Ther 2007;6:1683–91. [PubMed: 17541031]
27. Isoyama S, Dan S, Nishimura Y, Nakamura N, Kajiwara G, Seki M, et al. Establishment of phosphatidylinositol 3-kinase inhibitor-resistant cancer cell lines and therapeutic strategies for overcoming the resistance. Cancer Sci 2012;103:1955–60. [PubMed: 22925034]
28. Rebucci M, Peixoto P, Dewitte A, Wattez N, De Nuncques MA, Rezvoy N, et al. Mechanisms underlying resistance to cetuximab in the HNSCC cell line: role of AKT inhibition in bypassing this resistance. Int J Oncol 2011;38:189–200. [PubMed: 21109940]
29. Sen M, Joyce S, Panahandeh M, Li C, Thomas SM, Maxwell J, et al. Targeting Stat3 abrogates EGFR inhibitor resistance in cancer. Clin Cancer Res 2012;18:4986–96. [PubMed: 22825581]
30. Hasina R, Mollberg N, Kawada I, Mutreja K, Kanade G, Yala S, et al. Critical role for the receptor tyrosine kinase EPHB4 in esophageal cancers. Cancer Res 2013;73:184–94. [PubMed: 23100466]
31. Szwajda A, Gautam P, Karhinen L, Jha SK, Saarela J, Shakyawar S, et al. Systematic mapping of kinase addiction combinations in breast cancer cells by integrating drug sensitivity and selectivity profiles. Chem Biol 2015;22:1144–55. [PubMed: 26211361]
32. YoonH Dehart JP, Murphy JM Lim ST. Understanding the roles of FAK in cancer: inhibitors, genetic models, and new insights. J Histochem Cytochem 2015;63:114–28. [PubMed: 25380750]
33. Stabile LP, Egloff AM, Gibson MK, Gooding WE, Ohr J, Zhou P, et al. IL6 is associated with response to dasatinib and cetuximab: phase II clinical trial with mechanistic correlatives in cetuximab-resistant head and neck cancer. Oral Oncol 2017;69:38–45. [PubMed: 28559019]
34. Argiris A, Lee SC, Feinstein T, Thomas S, Branstetter BFt, Seethala R, et al. Serum biomarkers as potential predictors of antitumor activity of cetuximab-containing therapy for locally advanced head and neck cancer. Oral Oncol 2011;47:961–6. [PubMed: 21889392]
35. Caudell JJ, Sawrie SM, Spencer SA, Desmond RA, Carroll WR, Peters GE, et al. Locoregionally advanced head and neck cancer treated with primary radiotherapy: a comparison of the addition of

cetuximab or chemotherapy and the impact of protocol treatment. Int J Radiat Oncol Biol Phys 2008;71:676–81. [PubMed: 18355979]

36. Hu MH, Wang LW, Lu HJ, Chu PY, Tai SK, Lee TL, et al. Cisplatin-based chemotherapy versus cetuximab in concurrent chemoradiotherapy for locally advanced head and neck cancer treatment. Biomed Res Int 2014;2014:904341.
37. Strom TJ, Trotti AM, Kish J, Russell JS, Rao NG, McCaffrey J, et al. Comparison of every 3 week cisplatin or weekly cetuximab with concurrent radiotherapy for locally advanced head and neck cancer. Oral Oncol 2015;51:704–8. [PubMed: 25936651]
38. Nien HH, Sturgis EM, Kies MS, El-Naggar AK, Morrison WH, Beadle BM, et al. Comparison of systemic therapies used concurrently with radiation for the treatment of human papillomavirus-associated oropharyngeal cancer. Head Neck 2016;38 Suppl 1:E1554–61. [PubMed: 26595157]
39. Ley J, Mehan P, Wildes TM, Thorstad W, Gay HA, Michel L, et al. Cisplatin versus cetuximab given concurrently with definitive radiation therapy for locally advanced head and neck squamous cell carcinoma. Oncology 2013;85:290–6. [PubMed: 24217231]
40. Ye AY, Hay JH, Laskin JJ, Wu JS, Ho CC. Toxicity and outcomes in combined modality treatment of head and neck squamous cell carcinoma: cisplatin versus cetuximab. J Cancer Res Ther 2013;9:607–12. [PubMed: 24518704]
41. Huang J, Baschnagel AM, Chen P, Gustafson G, Jaiyesmi I, Folbe M, et al. Amatched-paircomparisonofintensity-modulatedradiationtherapywith cetuximab versus intensity-modulated radiation therapy with platinum-based chemotherapy for locally advanced head neck cancer. Int J Clin Oncol 2014;19:240–6. [PubMed: 23479120]
42. Tang C, Chan C, Jiang W, Murphy JD, von Eyben R, Colevas AD, et al. Concurrent cetuximab versus platinum-based chemoradiation for the definitive treatment of locoregionally advanced head and neck cancer. Head Neck 2015;37:386–92. [PubMed: 24431011]
43. Levy A, Blanchard P, Bellefqih S, Brahimi N, Guigay J, Janot F, et al. Concurrent use of cisplatin or cetuximab with definitive radiotherapy for locally advanced head and neck squamous cell carcinomas. Strahlenther Onkol 2014;190:823–31. [PubMed: 24638267]
44. Ou D, Levy A, Blanchard P, Nguyen F, Garberis I, Casiraghi O, et al. Concurrent chemoradiotherapy with cisplatin or cetuximab for locally advanced head and neck squamous cell carcinomas: Does human papilloma virus play a role? Oral Oncol 2016;59:50–7. [PubMed: 27424182]
45. Rawat S, Ahlawat P, Kakria A, Kumar G, Rangaraju RR, Puri A, et al. Comparison between weekly cisplatin-enhanced radiotherapy and cetuximab-enhanced radiotherapy in locally advanced head and neck cancer: first retrospective study in Asian population. Asia Pac J Clin Oncol 2017;13:195–203. [PubMed: 27813277]
46. Koutcher L, Sherman E, Fury M, Wolden S, Zhang Z, Mo Q, et al. Concurrent cisplatin and radiation versus cetuximab and radiation for locally advanced head-and-neck cancer. Int J Radiat Oncol Biol Phys 2011;81:915–22. [PubMed: 20947269]
47. Shapiro LQ, Sherman EJ, Riaz N, Setton J, Koutcher L, Zhang Z, et al. Efficacy of concurrent cetuximab vs. 5-fluorouracil/carboplatin or high-dose cisplatin with intensity-modulated radiation therapy (IMRT) for locally-advanced head and neck cancer (LAHNSCC). Oral Oncol 2014;50:947–55. [PubMed: 25132089]
48. Riaz N, Sherman E, Koutcher L, Shapiro L, Katabi N, Zhang Z, et al. Concurrent chemoradiotherapy with cisplatin versus cetuximab for squamous cell carcinoma of the head and neck. Am J Clin Oncol 2016;39: 27–31. [PubMed: 24401670]
49. Leeman JE, Li JG, Pei X, Venigalla P, Zumsteg ZS, Katsoulakis E, et al. Patterns of treatment failure and postrecurrence outcomes among patients with locally advanced head and neck squamous cell carcinoma after chemoradiotherapy using modern radiation techniques. JAMA Oncol 2017;3:1487–94. [PubMed: 28542679]
50. Perisanidis C. Prevalence of EGFR tyrosine kinase domain mutations in head and neck squamous cell carcinoma: cohort study and systematic review. InVivo 2017;31:23–34.
51. Licitra L, Mesia R, Rivera F, Remenar E, Hitt R, Erfan J, et al. Evaluation of EGFR gene copy number as a predictive biomarker for the efficacy of cetuximab in combination with chemotherapy

in the first-line treatment of recurrent and/or metastatic squamous cell carcinoma of the head and neck: EXTREME study. Ann Oncol 2011;22: 1078–87. [PubMed: 21048039]

52. Ang KK, Zhang Q, Rosenthal DI, Nguyen-Tan PF, Sherman EJ, Weber RS, et al. Randomized phase III trial of concurrent accelerated radiation plus cisplatin with or without cetuximab for stage III to IV head and neck carcinoma: RTOG 0522. J Clin Oncol 2014;32:2940–50. [PubMed: 25154822]
53. Smith ML, Arain AN, Herman TS, Bogardus CR Jr, Matthiesen CL, Thomp¬son JS. Cisplatin versus cetuximab combined with radiation therapy for definitive management of locally advanced squamous cell carcinoma of the head and neck: a matched cohort retrospective analysis. Int J Radiat Oncol Biol Phys 2015;93:E344.
54. UK CR [homepage on the Internet]. De-ESCALaTE determination of epidermal growth factor receptor-inhibitor (cetuximab) versus standard chemotherapy (cisplatin) early and late toxicity events in human papillomavirus-positive oropharyngeal squamous cell carcinoma 2013 Available from: https://clinicaltrials.gov/ct2/show/NCT01874171.
55. Group RTO [homepage on the Internet]. RTOG 1016 phase III trial of radiotherapy plus cetuximab versus chemoradiotherapy in HPV-associated oropharynx cancer 2011 Available from: https://clinicaltrials.gov/ct2/show/NCT01302834.
56. Group T-TRO [homepage on the Internet].TROG 12.01 a randomized trial of weekly cetuximab and radiation versus weekly cisplatin and radiation in good prognosis locoregionally advanced HPV-associated oropharyngeal squamous cell carcinoma 2013 Available from: https://clinicaltrials.gov/ct2/show/NCT01855451.
57. Harari PM, Harris J, Kies MS, Myers JN, Jordan RC, Gillison ML, et al. Postoperative chemoradiotherapy and cetuximab for high-risk squamous cell carcinoma of the head and neck: radiation therapy oncology group RTOG-0234. J Clin Oncol 2014;32:2486–95. [PubMed: 25002723]
58. Cancer Genome Atlas N. Comprehensive genomic characterization of head and neck squamous cell carcinomas. Nature 2015;517:576–82. [PubMed: 25631445]
59. Pickering CR, Zhang J, Yoo SY, Bengtsson L, Moorthy S, Neskey DM, et al. Integrative genomic characterization of oral squamous cell carcinoma identifies frequent somatic drivers. Cancer Discov 2013;3: 770–81. [PubMed: 23619168]
60. Chang KP, Wang CI, Pickering CR, Huang Y, Tsai CN, Tsang NM, et al. Prevalence of promoter mutations in the TERT gene in oral cavity squamous cell carcinoma. Head Neck 2017;39:1131–7. [PubMed: 28230921]
61. Foy JP, Pickering CR, Papadimitrakopoulou VA, Jelinek J, Lin SH, William WN Jr, et al. New DNA methylation markers and global DNA hypomethylation are associated with oral cancer development. Cancer Prev Res (Phila) 2015;8:1027–35. [PubMed: 26342026]
62. Sandulache VC, Michikawa C, Kataria P, Gleber-Netto FO, Bell D, Trivedi S, et al. High-risk TP53 mutations are associated with extranodal extension in oral cavity squamous cell carcinoma. Clin Cancer Res 2018;24:1727–33. [PubMed: 29330202]

Translational Relevance

Development of therapeutic resistance poses a challenging problem and limits the success of effective cancer therapies in the clinic. Cetuximab, an EGFR-specific antibody, is currently used with radiation for locally advanced head and neck cancer patients. However, 5-year survival rates remain low. We postulate that dysregulated levels of Eph-ephrin proteins play a compensatory role in bypassing the therapeutic effects mediated by anti-EGFR therapeutics. Our data demonstrate that targeted inhibition of EphB4–ephrin-B2 enhances sensitivity of patient-derived head and neck tumors toward cetuximab-radiotherapy. This enhanced radiosensitization effect is coupled with improved survival associated with decreased tumor cell proliferation and increased apoptosis. Our findings provide an insight into how blockade of EphB4–ephrin-B2 works in concert with EGFR inhibition to maximize therapeutic response to cetuximab-radiation treatment. The biological and therapeutic implications of this study hold promise for clinical translation in patients with locally advanced, EGFR-driven head and neck cancer.

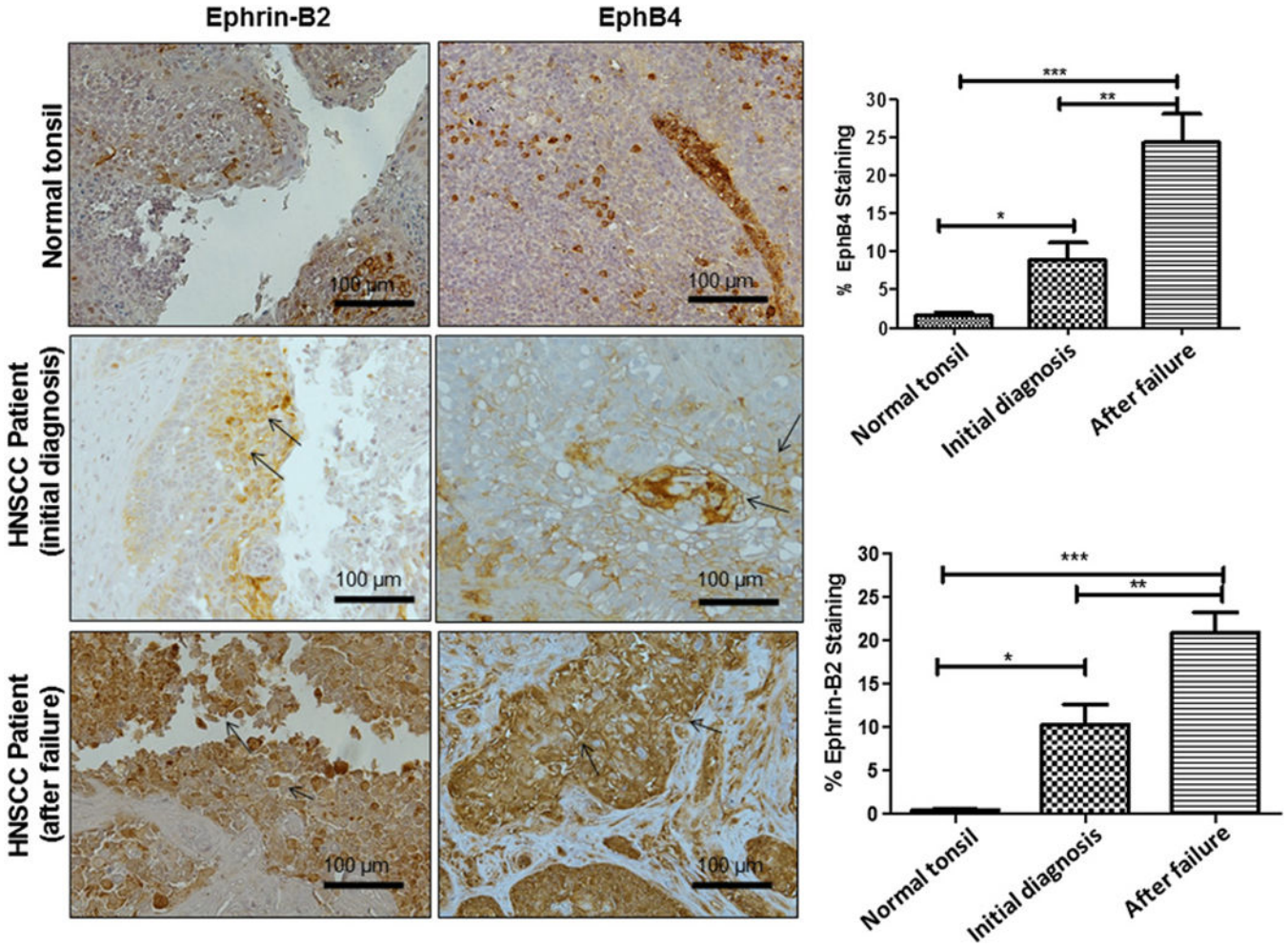

Figure 1.

EphB4 and ephrin-B2 are upregulated in HNSCC patients after failure following concurrent chemo and RT. We examined tumor samples biopsied from HNSCC patients (i) at the time of the first surgery before treatment with chemo-RT, and (ii) at the time of the second salvage surgery after they had chemo-RT failure and disease recurrence. We made a comparison of tissue within a group taken at the time of initial diagnosis and then after local failure, at the time of the salvage surgical procedure. Both EphB4 and ephrin-B2 are expressed in epithelial cells, stroma, and blood vessels in HNSCC patient tissue. In normal tonsil, ephrin-B2 is predominantly present in vessels and circulating immune cells. EphB4 is expressed at very low levels in normal epithelium. Quantitative IHC analysis shows predominantly high levels of EphB4 and ephrin-B2 in patients after treatment failure compared with the specimens biopsied at the time of initial diagnosis. Arrows represent positive signal on the EphB4 and ephrin-B2-stained tumor section. Total magnification: 200×. *, $P < 0.05$; **, $P < 0.005$; ***, $P < 0.0005$ are considered significant.

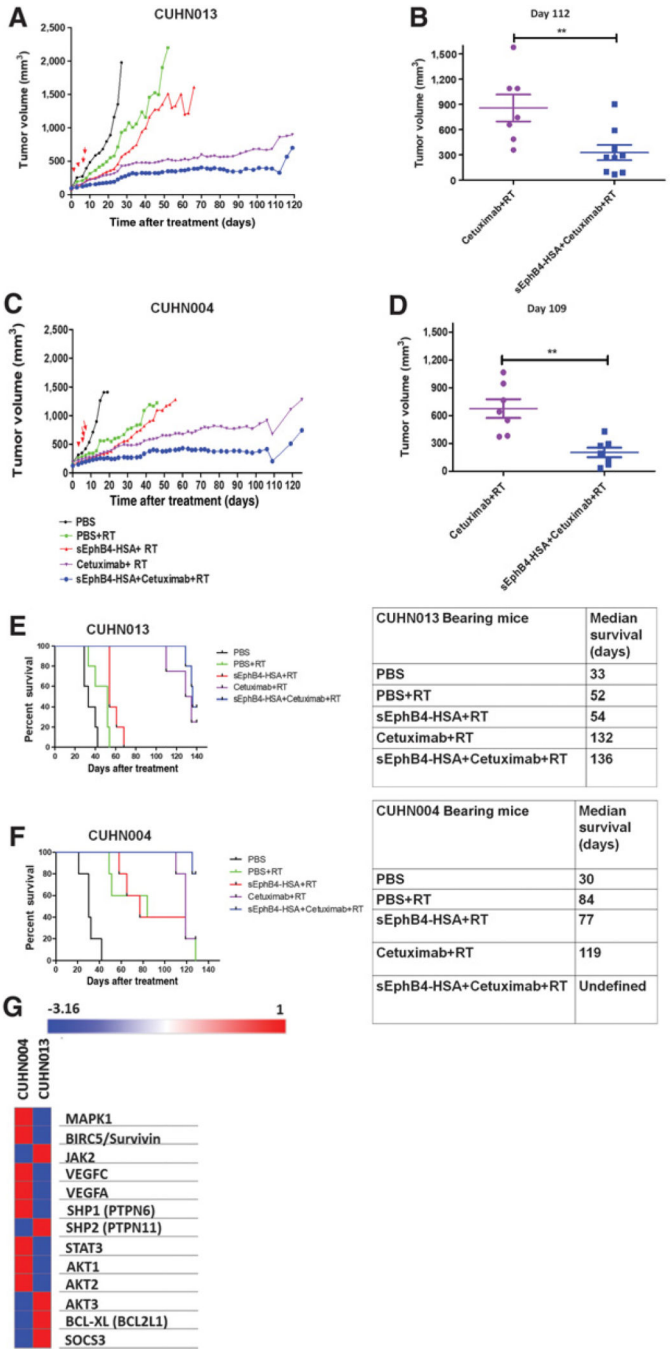

CUHN013 Bearing mice	Median survival (days)
PBS	33
PBS+RT	52
sEphB4-HSA+RT	54
Cetuximab+RT	132
sEphB4-HSA+Cetuximab+RT	136

CUHN004 Bearing mice	Median survival (days)
PBS	30
PBS+RT	84
sEphB4-HSA+RT	77
Cetuximab+RT	119
sEphB4-HSA+Cetuximab+RT	Undefined

Figure 2.

Inhibition of EphB4–ephrin-B2 signaling enhances response to EGFR inhibitor (cetuximab) and RT, resulting in significant delay in tumor growth and improved survival in HNSCC PDX models. Mice implanted subcutaneously with PDX tumors were randomized into different treatment cohorts. Tumor volumes are shown temporally for CUHN013 (**A**) and CUHN004 mice (**C**).Tumor volumes are also compared between cetuximab + RT and sEphB4-HSA + cetuximab + RT at day 112 (**B**) in CUHN013 mice and at day 109 posttreatment (**D**) for CUHN004 mice. Both tumor types showed significant decline when

EphB4–ephrin-B2 inhibitor was added to the cetuximab + RT arm. Kaplan-Meier survival curves show that in CUHN013 tumors, there is a significant increase in survival ingroups that received sEphB4-HSA + cetuximab + RT compared with sEphB4-HSA + RT or PBS + RT. There was no significant difference in terms of local tumor growth control in CUHN013 tumors subjected to triple combination sEphB4-HSA + cetuximab + RT compared with cetuximab-RT (**E**). CUHN004 tumors, on the other hand, showed a significant increase in survival in mice administered triple-combination treatment comprising cetuximab compared with others (**F**). **, $P < 0.005$; ***, $P < 0.0005$ are considered significant. **G,** mRNA sequencing was performed on CUHN013 and CUHN004 tumors to compare basal levels of gene expression. A heat map was generated using GeneE software (Broad Institute).

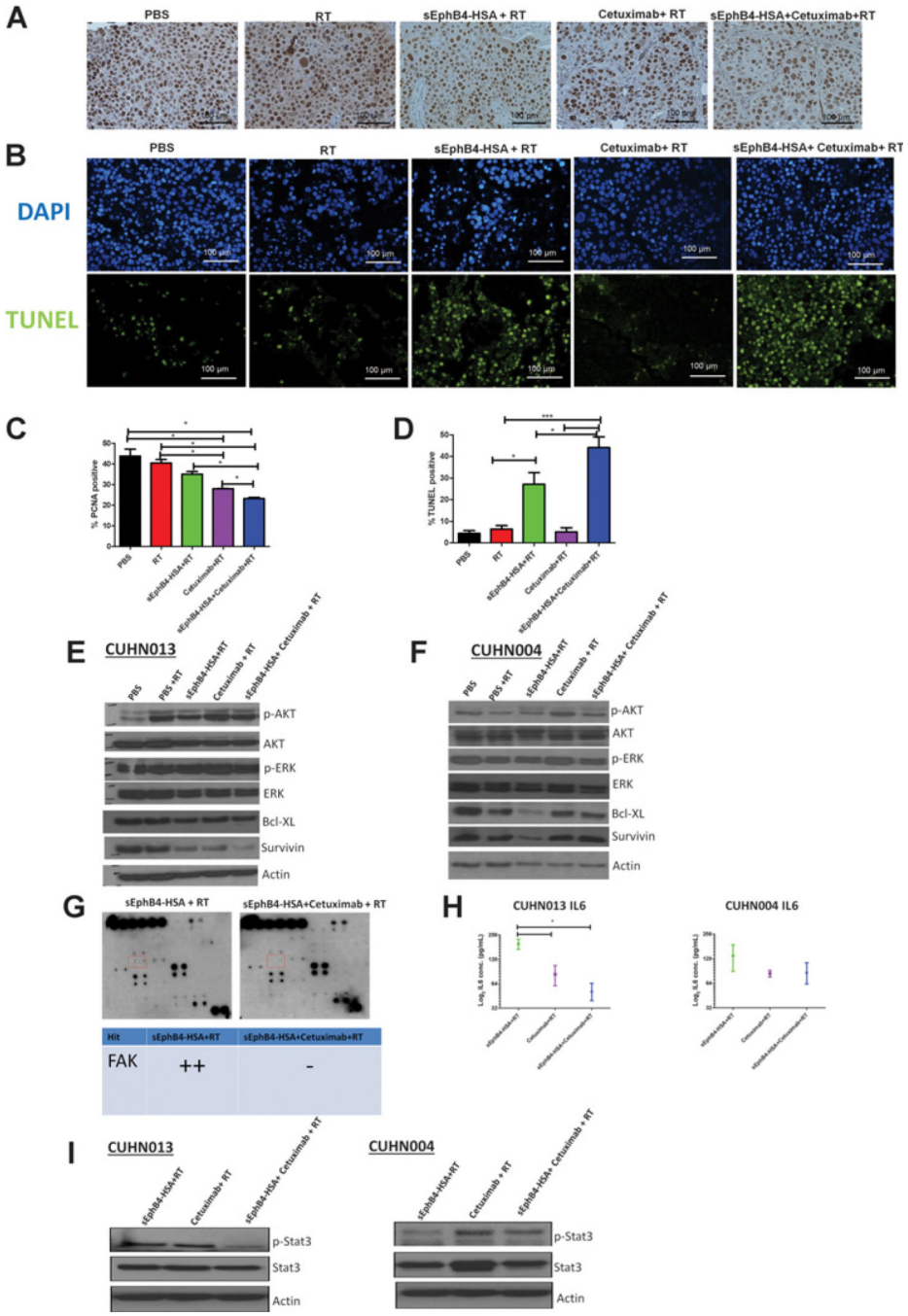

Figure 3.

Antitumor response observed in the EphB4–ephrin-B2 inhibition group with cetuximab and RT is associated with alteration in protein levels of key proliferation and survival molecules. IHC analysis showed a significant decrease in expression of PCNA, a proliferation marker, in CUHN013 tumors subjected to triple combination strategy compared with other experimental or control groups. PCNA staining (**A, C**) and TUNEL staining (**B, D**) were performed on tumors harvested from control and experimental groups. Data show a decrease in the percentage of PCNA-positive cells (**C**) and an increase in the number of TUNEL-

positive cells in sEphB4-HSA-cetuximab-RT compared with other cohorts (**D**). In addition, Western blot analysis performed on CUHN013 (**E**) showed a decrease in the levels of p-ERK, ERK, and survivin following EphB4–ephrin-B2 inhibitor treatment with cetuximab and RT. In CUHN004 tumors (**F**) p-AKT, p-ERK, ERK, and Bcl-XL were mainly affected following triple combination treatment with cetuximab. Samples from control and experimental groups were run together on the same gel. Phospho-RTK array was performed on CUHN013 tumors that were subjected to sEphB4-HSA + RT, or sEphB4-HSA + cetuximab + RT treatments. Data indicate a decrease in the levels of p-FAK in the triple combination treatment compared with its respective control (**G**). Plasma samples were collected from PDX tumor-bearing mice at 96 hours after RT and subjected to U-plex assay. Decrease in the levels of IL6 was prominent in CUHN013 tumors that received sEphB4-HSA inhibitor in combination with cetuximab-RT compared with others (**H**). Western blot analysis for p-STAT3 mirrored the IL6 trend in CUHN013 tumors and showed reduction in the levels of p-STAT3 in sEphB4-HSA + cetuximab + RT compared with other groups (**I**). *, $P < 0.05$; ***, $P < 0.0005$ are considered significant. Total magnification, x200.

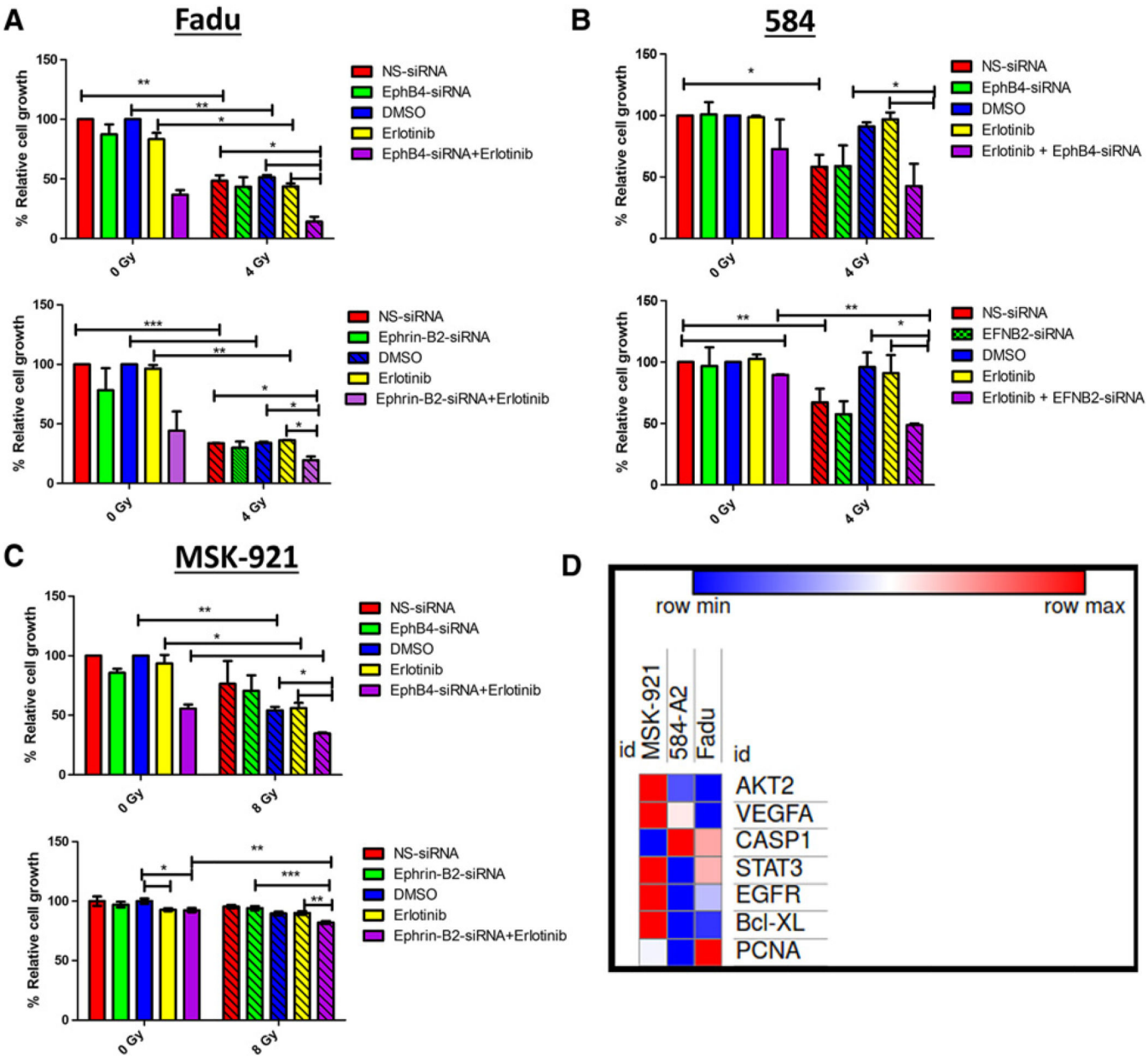

Figure 4.

Combined EphB4/ephrin-B2 and EGFR inhibition results in decreased tumor cell growth in the presence of radiation *in vitro*. Decreased tumor cell growth is observed in Fadu (**A**), 584 (**B**), and MSK-921 (**C**) cells as analyzed by MTT assay at 96–120 hours after RT in the EphB4/ephrin-B2 silenced groups when combined with the EGFR inhibitor (60 nmol/L) and RT. Each group had at least 6 replicates. Error bars, mean ± SD or mean ± SE. *, $P < 0.05$; **, $P < 0.005$; ***, $P < 0.0005$ are considered significant. **D**, Heat map generated based on microarray data analysis showing a differential pattern of expression of genes involved in tumor growth, proliferation, survival, and therapeutic resistance. Comparisons are made between MSK-921, Fadu, and 584 cell lines.